ment. Typical probes had wire diameters from 0.001 to 0.0025 cm, coil diameters from 0.010 to 0.013 cm, and wire (l/d)'s from 400 to 1500.

Probes were calibrated in two facilities using helium as a test medium. The first facility was a 7.6-cm exit diameter conical nozzle which had a stream Mach number near 20. The second facility was a low-density nozzle which had a stream Mach number near 4. A description of the flow conditions of these nozzles can be found in Ref. 2. The probe calibration and data reduction procedures were essentially identical to those of Ref. 1.

Typical calibrations for Nu_t against $Re_{t,d}$ and η against $Re_{t,D}$ are shown in Fig. 2a and 2b, respectively. In Fig. 2a, Nu_t and $Re_{t,d}$ were based on wire dimensions, since the heat transfer took place on the wire surface. Data from a coiled wire are given by the open symbols. The same data with calculated end losses removed are shown by solid symbols. The slope of the corrected data is 0.91, and is typical for the coil probes examined. A calibration curve for a conventional probe from Ref. 1 was corrected for end losses and is shown for comparison. The conventional probe calibration curve has a similar level but a smaller slope than that for the coiled probe. This may be due to the different local flows around the two probes. The coil probe recovery factor corrected for end loss is shown in Fig. 2b for two different (l/d)'s. The recovery factor is shown against $Re_{t,D}$ along with a fairing of recovery factor data for a straight cylinder with end loss effects removed.[3] The value of η for both (l/d)'s agrees with the data of Ref. 3 indicating that the probe shock was probably detached ahead of the entire coil rather than each wire loop. The fairing from the data of Ref. 3 is given here by the dashed line for comparison.

Experimental Studies Using Coil Probes

The nozzle wall boundary layer in the 7.6 cm, $M \simeq 20$ facility is turbulent at higher operating pressures[4] and radiates sound into the freestream flow.[5] When a new design probe is tested in this nozzle, the fluctuation spectrum obtained can be compared with that of conventional hot wires to determine response characteristics. The freestream disturbance spectrum obtained with a long wire ($l/d = 1500$) coil probe in this facility is shown in Fig. 3. The spectrum from a conventional wire[4] is also shown in Fig. 3 for comparison. The spectrum was the same as that of the conventional wire except for a small spike at $\simeq 5$ KHz. The spike was evidently caused by a resonant vibration of the coil at this frequency. The effect of this spike is generally small and can be neglected for either mean flow measurements or wide band fluctuation measurements. However, for some cases, this vibration may have to be considered (e.g., narrow band measurements near the resonant frequency).

To further check the probe accuracy, mean boundary-layer measurements were obtained on a cone in the Langley $M_\infty \simeq 20$ High Reynolds number helium tunnel using the coil probes. Details of the facility can be found in Ref. 6. The boundary layer on the cone (cone half angle = 2.87° cone at $3\frac{1}{2}$° angle of attack) was probed with both a pitot probe and a coil probe to determine 3-D transitional and turbulent boundary-layer profiles at a local Mach number of $\simeq 10$. Since the model wall temperature was near the flow total temperature, the pitot data was reduced by assuming constant total temperature. The hot-wire temperature survey verified that the total temperature variation through the boundary layer was less than 5%. Typically mass flow profiles obtained with both pitot probe and coil hot-wire probe showed agreement to within 4% throughout the entire boundary layer.

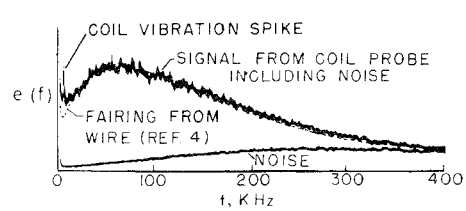

Fig. 3 Spectrum from hot-wire coil-probe in 7.6-cm helium nozzle.

In concluding, the coil hot-wire probe exhibits all the advantages of conventional hot-wire probes, and few of the disadvantages. Thus the coil probe is particularly useful for high-speed flow studies where probe breakage and large end loss errors are bothersome.

References

[1] Wagner, R. D., Jr., Maddalon, D. V., and Weinstein, L. M., "Influence of Measured Freestream Disturbances on Hypersonic Boundary-Layer Transition," *AIAA Journal*, Vol. 8, No. 9, Sept. 1970, pp. 1664–1670.

[2] Weinstein, L. M., "A Shielded Fine-Wire Probe for Rapid Measurement of Total Temperature in High Speed Flows," *Journal of Spacecraft and Rockets*, Vol. 8, No. 4, April 1971, pp. 425–428.

[3] Weltmann, R. N. and Kuhns, P. W., "Heat Transfer to Cylinders in Crossflow in Hypersonic Rarefied Gas Streams," TN D-267, March 1960, NASA.

[4] Weinstein, L. M., "Effect of Oblique Shock on Free Stream Disturbances at $M_\infty \simeq 20$ in Helium," Masters thesis, 1972, George Washington Univ., Washington, D.C.

[5] Laufer, J., "Aerodynamic Noise in Supersonic Wind Tunnels," *Journal of the Aerospace Sciences*, Vol. 28, No. 9, Sept. 1961, pp. 685–692.

[6] Watson, R. and Bushnell, D. M., "Calibration of the Langley Mach 20 High Reynolds Number Helium Tunnel Including Diffuser Measurements," TM X-2353, Oct. 1971, NASA.

Design of Least Weight Structures for Prescribed Buckling Load

KALAYYA NARAYANA MURTHY* AND PAUL CHRISTIANO†
University of Minnesota, Minneapolis, Minn.

1. Introduction

DESPITE the significant effort of the past decade directed toward advancing analytical techniques for optimal design of single-span columns, optimization of complex structures under prescribed buckling load using numerical methods has apparently not been reported. However, using various discretization procedures, considerable attention has been paid to the nearly equivalent mathematical problem involving the design of structures subject to a frequency constraint. Of these procedures, the gradient method of Zarghamee[1] and Rubin[2] seems to be well suited for extension to buckling problems. Whereas the method originally comprised a finite element formulation in which only a linear weight-stiffness relationship was considered, here a quadratic relationship is used. Further, an averaging technique is described which permits the design parameter to vary uniformly over preassigned segments. The optimal design of a two-span continuous column is illustrated.

2. Optimization Method

The procedure begins with an initial design which is modified so as to satisfy the buckling load constraint; then, holding the buckling load constant, the weight is minimized.

Received May 29, 1973.
Index categories: Aircraft Structural Design (Including Loads); Structural Design, Optimal; Structural Stability Analysis.

* Graduate Student, Department of Civil and Mineral Engineering.
† Associate Professor, Department of Civil and Mineral Engineering.

The stability problem may be expressed as

$$[K]\{q\}-\lambda[S]\{q\}=0 \tag{1}$$

where λ represents the buckling load and $[K]$, $[S]$ and $\{q\}$ are the elastic stiffness matrix, stability matrix, and eigenvector of the system, respectively. Further

$$[K]=\sum_{i=1}^{m} a_i[k_i]+[\bar{K}]$$

and (2)

$$[S]=\sum_{i=1}^{m} N_i[S_i]+[\bar{S}]$$

where a_i, N_i, and $a_i[k_i]$ and $N_i[S_i]$ are, respectively, the stiffness parameter, membrane or axial force, elastic stiffness matrix, and stability matrix for the ith variable element, of which there are m number. $[\bar{K}]$ and $[\bar{S}]$ represent matrices for that portion of the structure which undergoes no change during redesign.

The elemental stiffness parameter a_i and weight w_i may be related to the ith design parameter d_i by

$$\begin{aligned} a_i &= \xi_1 d_i+\xi_2 {d_i}^2+\dots \\ w_i &= \zeta\rho L_i d_i \end{aligned} \tag{3}$$

where ξ_1, ξ_2, and ζ are constants for a given cross-sectional shape, ρ is the constant weight per unit volume, and L_i is the characteristic length or area of the ith element.

By determining the gradient of λ relative to the design parameters $d_1,\dots,d_m$, and neglecting the effect of self-weight, the change in the ith parameter Δd_i due a change in the eigenvalue $\Delta\lambda$ is, to a linear approximation

$$\Delta d_i=\Delta\lambda\frac{\lambda_{,i}}{\Phi_i}\sum_{j=1}^{m}\frac{\Phi_j}{{\lambda_{,j}}^2} \tag{4}$$

where

$$\lambda_{,i}=\{q\}^T[K]_{,i}\{q\} \tag{5}$$

and is the ith component of $\{\nabla\lambda\}$ (subscript $,i$ designates $\partial/\partial d_i$), and $\Phi_i=w_{i,i}=\zeta\rho L_i$. The change in structural weight is then

$$\Delta W=\sum_{i=1}^{m}\Phi_i\Delta d_i \tag{6}$$

Given an admissible trial design, the actual buckling load λ and corresponding eigenvector are found from Eq. (1). As the structure is to be modified to meet a prescribed buckling load λ_p, the difference between λ and λ_p is decreased in small increments $\Delta\lambda$ [in keeping with the limitations of Eq. (4)]; for each increment, Δd_i and ΔW are computed using Eqs. (4) and (6). If initially $\lambda<\lambda_p$, the procedure permits λ to approach λ_p with a minimum of additional weight. This phase of the process is terminated when $\lambda\simeq\lambda_p$ to within some prescribed tolerance (here taken as $0.01\lambda_p$).

The weight-minimization phase is based on the condition that prior to achieving an optimal design a change in the set of design parameters may be chosen with no reduction in buckling strength, or

$$\Delta\lambda=\sum_{i=1}^{m}\Delta d_i\lambda_{,i}\equiv 0 \tag{7}$$

To satisfy Eq. (6), it is possible to prescribe Δd_i for only $(m-1)$ variable elements; for the remaining mth element, it is necessary that

$$\Delta d_m=\frac{1}{\lambda_{,m}}\sum_{i=1}^{m-1}\Delta d_i\lambda_{,i} \tag{8}$$

Consequently, the negative change in weight is

$$-\Delta W=\sum_{i=1}^{m-1}\Delta d_i\sigma_i \tag{9}$$

where

$$\sigma_i=\Phi_m\lambda_{,i}/\lambda_{,m}-\Phi_i \tag{10}$$

Assuming Δd_i to be taken as

$$\Delta d_i=\Omega(\sigma_i/\Phi_i) \tag{11}$$

leads to

$$-\Delta W=\Omega\sum_{i=1}^{m-1}\frac{{\sigma_i}^2}{\Phi_i} \tag{12}$$

where Ω is a proportionality constant. When an optimal design is attained, $-\Delta W\equiv 0$, and consequently, Eqs. (9) and (10) lead to the optimality condition

$$\lambda_{,i}/\Phi_i=\lambda_{,m}/\Phi_m \tag{13}$$

For each variable element comprising the optimal shape, the quantity on either side of Eq. (13) equals the same constant. This implies that for a linear weight-stiffness relationship the strain energy per unit length or area is constant for all varible elements.

To approach the optimal design incrementally, a reduction in weight is attempted by specifying $-\Delta W\ll W$ in Eq. (12) and solving for Ω; resulting changes in the design variables and buckling load are found from Eqs. (11, 8, and 7) using Eqs. (10) and (5). The iteration process is terminated when an arbitrarily small reduction in W causes an excessive change in λ. At this point Eq. (13) is very nearly satisfied.

As fabrication of structures with a large number of variable sections is usually impractical, it is often desirable to allow the cross-sectional area to be constant in certain preassigned segments. This problem has been considered in previous analytical investigations[3,4] not dealing with buckling problems. Accommodation is made here by considering the change in design parameter in a uniform segment to be proportional to the root-mean-square of $(\lambda_{,i}/\Phi_i)$ for the elements comprising the segment; that is, over the segment composed of elements k through $(k+l)$

$$\Delta {d_k}^{k+l}=\Delta\lambda\frac{\left[\sum_{i=k}^{k+l}(\lambda_{,i}/\Phi_i)^2\right]^{1/2}}{(l)^{1/2}\sum_{i=1}^{m}({\lambda_{,i}}^2/\Phi_i)} \tag{14}$$

If all the elements in the segment are of constant length, then Φ_i is the same for each element and cancels out of the foregoing expression.

3. Numerical Examples

Example a

As a means of estimating accuracy, the method is applied to a hinged-clamped column under constant axial force, and results are compared with the analytical solution of Tadjbakhsh and Keller,[5] assuming moment of inertia to be related to the square of the design parameter (here the cross-sectional area). Figure 1 shows a fairly good comparison between weight or volume distributions of the analytical solution and the numerical solution employing 20 beam-column elements of equal length. The cross-sectional area $A(\bar{x})$ is normalized relative to the average area V/L (V = total volume and L = length of member).

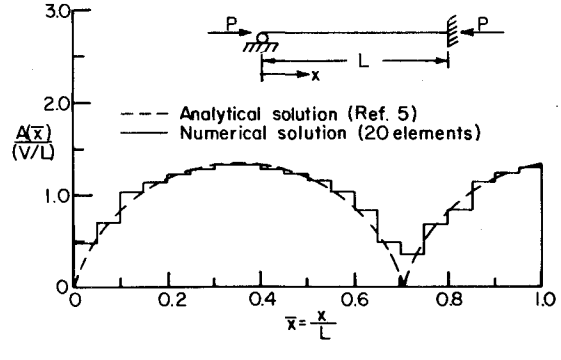

Fig. 1 Comparison of numerical and analytical solutions.

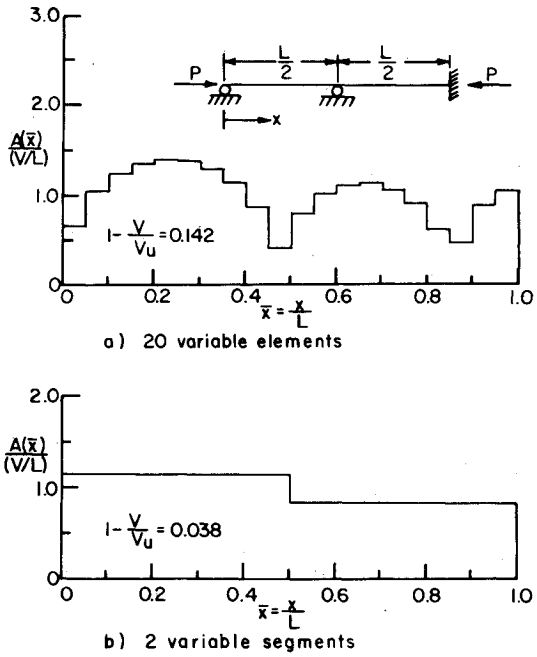

Fig. 2 Optimum shape of a continuous beam.

V_u is the volume of the uniform column having the same buckling load. The savings in weight over a uniform column of equal buckling strength is 12.8% with the present method compared with 14.0% obtained from the analytical solution. The initial design was taken as a uniform column having a buckling strength equal to 10% of the prescribed value; using a CDC 6600, CP time was 23 sec.

Example b

The second example is a continuous column having hinged-clamped outer supports and a roller at midspan. Considering the axial force to be constant, and taking the same weight-stiffness relationship as in the previous example, the optimal material distribution is as indicated in Fig. 2. The results of allowing each of the 20 elements to vary independently is shown in Fig. 2a. The savings in weight over a uniform column of equal strength is 14.2%. By forcing all the elements in each span to maintain the same cross section, the volume distribution is that shown in Fig. 2b; the material savings is 3.8%. It should be mentioned that if the structure were represented by only one element per span, the model would lead to large inaccuracies. The buckling load for such a model, e.g., is 28.9% in excess of the exact value; subsequent optimization would, therefore, incorrectly imply a material savings of 36.8%, which represents a large unconservative error.

References

[1] Zarghamee, M. S., "Optimum Frequency of Structures," *AIAA Journal*, Vol. 6, No. 4, April 1968, pp. 749–750.

[2] Rubin, C. P., "Minimum Weight Design of Complex Structures Subject to a Frequency Constraint," *AIAA Journal*, Vol. 8, No. 5, May 1970, pp. 923–927.

[3] Sheu, C. Y. and Prager, W., "Minimum Weight Design with Piecewise Constant Specific Stiffness," *Journal of Optimization Theory and Applications*, Vol. 2, No. 3, March 1968, pp. 179–186.

[4] Chern, J. M. and Prager, W., "Optimal Design of Beams for Prescribed Compliance Under Alternate Loads," *Journal of Optimization Theory and Applications*, Vol. 5, No. 6, June 1970, pp. 425–431.

[5] Tadjbakhsh, I. and Keller, J. B., "Strongest Columns and Isoperimetric Inequalities for Eigenvalues," *Journal of Applied Mechanics*, Vol. 29, No. 1, March 1962, pp. 159–164.

Reflectance and Unsteady Temperature Distribution of Diffuse Reflectors

KENNETH C. WESTON* AND R. S. REDDY†
University of Tulsa, Tulsa, Okla.

THE applicability of the Kubelka-Munk two flux approach to the estimation of the temperature distribution in volume reflectors was pointed out in Ref. 1. There an historic exact solution of the Kubelka-Munk equations for the reflectance of an absorbing and scattering material was presented. A reflectance solution of the Kubelka-Munk equations for the case of zero absorption coefficient was also presented and applied to the problem of the calculation of steady-state temperature distributions in volume reflectors. The adequacy of the zero absorption coefficient solution for the approximation of the reflectance of a weakly absorbing, highly scattering material is considered here. A solution for the transient heating of a one-dimensional volume reflector is given. The effect of the error incurred in employing the zero absorption equation for the estimation of the transient heating of a volume reflector is then considered for early times appropriate to the entry heat protection system application.

Reflectance solutions of the Kubelka-Munk differential equations are expressed in terms of the ratio of absorption to scattering coefficient, k/s, the scattering power, $S = s\delta$, and the rear surface reflectance, R_B, where δ is the thickness of the one-dimensional volume reflector. The reflectance of a diffuser of infinite thickness is given by

$$R_\infty = 1 + k/s - [k/s(k/s+2)]^{1/2} \tag{1}$$

The reflectance of a thickness δ of this material backed with a material of reflectance R_B is then expressed in terms of R_∞ as

$$R = \frac{(1/R_\infty)(R_B - R_\infty) - R_\infty(R_B - 1/R_\infty)\exp[S(1/R_\infty - R_\infty)]}{(R_B - R_\infty) - (R_B - 1/R_\infty)\exp[S(1/R_\infty - R_\infty)]} \tag{2}$$

A solution of the Kubelka-Munk equations for $k = 0$ is also available:

$$R_{k=0} = [1-(1-R_B)(1-S)]/[1+(1-R_B)S] \tag{3}$$

These reflectance solutions are exact solutions of the Kubelka-Munk differential equations. The relative simplicity of Eq. (3) suggests that it may be more convenient to apply this equation as an approximation for weakly absorbing materials than Eq. (2). Such an application was made in Refs. 1 and 2. These solutions assume that internal emission is negligible for the weak absorption, moderate temperature conditions presumed here.

A comparison of Eqs. (2) and (3) is given in Fig. 1 for the case of $R_B = 0.95$ and a range of values of k/s and S. For the case of S approaching zero, the over-all reflectance tends towards the reflectance of the rear surface. For small values of k/s, it is evident that Eq. (2) indicates that increasing the scattering power increases the over-all reflectance due to the dominance of the scattering centers within the material. For values of k/s exceeding about 10^{-3}, it is seen that the reflectance falls below the back surface reflectance due to dominance of absorption processes within the material.

Of primary interest here are extremely low values of k/s which are characteristic of good diffuse reflectors. It is seen in Fig. 1 that the nonabsorbing solution given in Eq. (3) approximates, for these low k/s values, the reflectance of diffuse reflectors as characterized by Eq. (2). As an example, values of k and s have been estimated for fritted quartz in Ref. 2 to be $k = 0.005$ cm^{-1} and $s = 10$ cm^{-1}. For these values and a

Received May 31, 1973. This research has been partially supported under NASA Grant NGR 37-008-003.

Index categories: Entry Vehicles and Landers; Heat Conduction; Radiation and Radiative Heat Transfer.

* Associate Professor of Mechanical Engineering. Member AIAA.
† Graduate Research Assistant.